 CMES, vol.6, no.4, pp.373-395, 2004

PDE-Driven Level Sets, Shape Sensitivity and Curvature Flow for Structural Topology Optimization

Michael Yu Wang[1] **and Xiaoming Wang**[2]

Abstract: This paper addresses the problem of structural shape and topology optimization. A level set method is adopted as an alternative approach to the popular homogenization based methods. The paper focuses on four areas of discussion: (1) The level-set model of the structure's shape is characterized as a region and global representation; the shape boundary is embedded in a higher-dimensional scalar function as its "iso-surface." Changes of the shape and topology are governed by a partial differential equation (PDE). (2) The velocity vector of the Hamilton-Jacobi PDE is shown to be naturally related to the shape derivative from the classical shape variational analysis. Thus, the level set method provides a natural setting to combine the rigorous shape variations into the optimization process. (3) Perimeter regularization is incorporated in the method to make the optimization problem well-posed. It also produces an effect of the geometric heat equation, regularizing and smoothing the geometric boundaries as an anisotropic filter. (4)We further describe numerical techniques for efficient and robust implementation of the method, by embedding a rectilinear grid in a fixed finite element mesh defined on a reference design domain. This would separate the issues of accuracy in numerical calculations of the physical equation and in the level-set model propagation. Finally, the benefit and the advantages of the developed method are illustrated with several 2D examples that have been extensively used in the recent literature of topology optimization, especially in the homogenization based methods.

keyword: Topology optimization, level set method, shape sensitivity, curvature flow

[1] Department of Automation and Computer-Aided Engineering, The Chinese University of Hong Kong, Shatin, NT, Hong Kong. Tel.: +852-2609-8487; Fax: +852-2603-6002. E-mail: yuwang@acae.cuhk.edu.hk (M. Y. Wang).

[2] School of Mechanical Engineering Dalian University of Technology Dalian 116024, China

1 Introduction

Structural optimization, in particular the shape and topology optimization, has been identified as one of the most challenging tasks in structural design. Various techniques have been developed in the past decades. Typical procedures are based on an explicit boundary representation with a *fixed topology* of the structure (Bendsoe (1997); Rozvany (1998); Sokolowski *et al.* (1992)). In the direct approach, the problem of structural optimization is a *well-posed* mathematical problem, and numerical algorithms can be developed based on rigorous analyses for shape sensitivity and necessary optimality conditions (Haug *et al.* (1986); Sokolowski *et al.* (1992)). As a result, these optimization procedures are widely available in commercial finite element software systems. However, these procedures do not admit changes in the connectivity of the geometry of the structure, imposing a significant constraint on the design and thus limiting the potential of the structural performance. Perhaps as a major motivation to overcome the fixed-topology limitation, the concept of *topology optimization* has been introduced in recent years (Bendsoe (1989, 1997); Bendsoe *et al.* (1988, 1993)), often with a "raster" geometric model of a refined finite element grid covering the candidate design domain. Over the past decade, there have been some extensive developments of various approaches to this problem.

Unfortunately, the problem of topology optimization of a structure is an *ill-posed* problem in its mathematical theory and numerical methods (Haber *et al.* (1996)). As first observed numerically in (Cheng *et al.* (1981)) for a variable-thickness plate design problem, the optimization problem may not admit a solution. Particularly for the problem of minimizing the structural compliance of an elastic body for a specified set of loads and supports, it has been illustrated that a non-convergent design sequence can be constructed such that the compliance reduces monotonically (Bendsoe (1997)). The resulting

design has a configuration with an unbounded number of microscopic holes, rather than a finite number of macroscopic holes.

For the reason to generate a well-posed topology optimization problem, the so-called homogenization method has been extensively developed in recent years and evolved into the state-of-the-art (Bendsoe (1989, 1997); Bendsoe *et al.* (1988, 1993)). In this approach, the design space is first extended to explicitly include materials with periodic, perforated microstructures and then homogenization theory is utilized to compute effective material properties. This procedure is known as *relaxation* and, as a result, solutions to the relaxed problem are guaranteed to exist. A "side-effect" of the relaxation is that the optimal solutions generated by homogenization methods commonly have perforated microstructures in the resulting design, as expected in consistence with the relaxation. Unfortunately, perforated microstructures are difficult to manufacture. Thus, the "relaxed" optimal solutions may not lead directly to useful designs.

Therefore, it becomes necessary to be able to suppress perforated microstructures in the optimal design by modifying the relaxed formulation. Several suppression techniques have been developed. Introducing *a priori* restrictions on the configuration of the microstructure is an approach presented in (Bendsoe (1997); Bendsoe *et al.* (1988)), while the suppression may also be achieved by explicitly penalizing intermediate values of the bulk density. The later technique becomes quite popular, especially with the "solid isotropic material with penalization" (SIMP) approach for its conceptual and practical simplicity (Bendsoe (1997); Mlejnek (1992); Rozvany (2001)). It has been pointed out that certain configuration restrictions are equivalent to explicit penalties on intermediate densities (Bendsoe *et al.* (1999)), thus yielding similar designs. Various "*engineering approaches"* have also been suggested, including adding more constraints into the problem such as perimeter controls (Petersson (1999)) and slope constraints (Petersson *et al.* (1998)), and employing filters for chattering solutions (Bourdin (2001); Sigmund (2000, 2001); Sigmund *et al.* (1998); Wang and Zhou (2004); Tapp *et al.* (2004)). Although these suppression techniques have been widely applied to problems with multiple physics and multiple materials (Bendsoe (1997); Bourdin (2001); Bulman *et al.* (2001); Rozvany (2001); Suzuki et. al. (1991)), the solutions are often mesh dependent. Further, numerical instabilities are inherent and may introduce "non-physical" artifacts in the results to make the designs sensitive to variations in the physical and numerical parameters of the system such as loading (Bourdin (2001); Bulman *et al.* (2001); Rozvany (2001); Sigmund *et al.* (1998)). The suppressions do not directly address the chattering problem underlying the relaxation concept.

An alternative approach for generating a well-posed topology optimization problem is to define the design space to exclude chattering designs (Ambrosio *et al.* (1993); Larsen *et al.* (2001)). A common approach is to introduce an upper bound constraint on the perimeter of the design (Haber *et al.* (1995)). A numerical investigation of the "perimeter constraint method" was given in (Haber *et al.* (1995)), which shows that a perimeter constraint can effectively exclude perforated material and result in a well-posed macroscopic design. A more fundamental approach is to use the perimeter as a penalization for regularizing the ill-posedness of the topology optimization problem. A mathematical analysis of the *perimeter regularization method* was first presented in (Ambrosio *et al.* (1993)). Other studies also provide more mathematical support for the approach (Larsen *et al.* (2001)), which in fact has been extensively utilized in the field of digital image processing over the years (Sapiro (2001)).

Another essential feature of most of the existing topology optimization approaches is the *"raster" geometric model*. A finite element grid is used both for representing the structure and for physical analysis of the structural mechanics. In the final optimal design, an effective indicator value of either 0 or 1 (or in between) is obtained for each element to define the design geometry implicitly. In the end, the designer must interpret the resulting distribution and extract the boundaries of the solid region (Lin *et al.* (2000)). This is in contrast to the boundary models that are commonly used in finite element procedures for shape optimization. Boundary representations are always essential for design description and for design automation with CAD and CAE systems. These fundamental issues are still argued in the literature (Rozvany (2001)).

Adopting the same spirit of using boundary-representation geometric models, a new approach was recently proposed using the versatile level-set models (Osher *et al.* (2001); Sethian *et al.* (2000); Wang *et al.* (2003); Sheen *et al.* (2003)). The level

set method was developed in (Osher *et al.* (2003)) to provide an efficient way of describing time evolving curves and surfaces which may undergo topological changes. It has been recognized that the level-set models are well suited to the structural topology optimization, as they can form holes, split into multiple pieces, or merge with others to form a single one (Osher *et al.* (2001); Wang *et al.* (2003); Wang *et al.* (2004)). They are used in (Sethian *et al.* (2000)) to accommodate an evolutionary procedure of removing (or adding) material in regions according to the stress levels computed with an explicit jump immersed interface method without using meshes. The general topology optimization problem can be formulated as a problem of tracking the geometric boundaries as motion of level sets driven by the optimization conditions (Allaire *et al.* (2002); Wang *et al.* (2003); Wang *et al.* (2004)).

In this paper we address the topology optimization problem of a linearly elastic structure with the level-set formulation. For a given design objective and a set of constraints, a global minimization criterion is introduced, consisting of the design objective and a perimeter penalty proportional to the Hausdorff measure of the design boundary. In using the level-set model, the boundary of the structure is embedded in a scalar function of a higher dimensionality. Based on the level set theory, the dynamic change of the structural boundary is governed by a partial differential equation (PDE) of Hamilton-Jacobi type. Thus, the topology optimization is described as a solution of the Hamilton-Jacobi equation. More specifically, the paper focuses on the following three areas of discussions:

1. *Evolution of geometric boundary embedded in a higher-dimensional space*. The level set model is defined as a *region representation* of the structure's shape. A comprehensive understanding of the structural shape involves both the notions of its boundary *and* its interior. While the classical shape optimization has focused mainly on the process of changing the boundaries of the shape, the modern notion of topology optimization captures the regions bounded by the boundaries. The level set model provides this extra "dimension" of information by allowing for an evolution of the three-dimensional boundaries in a higher four-dimensional space constrained to embed the original problem. The permissible changes of the boundaries are further constrained by the dynamic motions of the level sets defined by their partial differential equations. Within this global and region-based framework, the topology optimization of the structure is transformed into a process of motion of the PDE-driven level-set.

2. *The velocity field in level-set evolution and the classical shape derivative*. We will further examine the role of the velocity field in the Hamilton-Jacobi equation and its relationship to the shape derivative of the classical shape optimization. We will show that the shape derivative defined in the framework of shape diffeomorphism is naturally associated with the flow of the velocity field of the evolution of the level set model. Thus, the level set representation can be naturally combined with an application of the classical shape analysis. Such a combination provides a proper and determinant choice of the velocity field to lead a convergent process of minimizing the objective functional.

3. *Perimeter regularization and curvature-based diffusion*. We will study the regularizing effect of the perimeter penalty for the topology optimization problem. The primary effect of a perimeter penalization is that it ensures the existence of smooth solutions. For the level set representation, this effect is shown to be equivalent to curvature diffusion. In other words, the regularization effect can be viewed as running the geometric shape through a nonlinear heat equation. Since the geometric heat equation may be regarded as a nonlinear Guassian smoothing process, the perimeter regularization can also be related to an anisotropic filtering which gives a number of advantages as widely used in imaging processing.

4. *Numerical computations for approximated solutions.* We shall describe numerical techniques for efficient and robust implementation of the proposed method. Since it is convenient to numerically solve the level set PDE with a fixed rectilinear spatial grid, we suggest that such a grid is embedded as nodes in a finite element mesh which is defined in a fixed reference domain for numerical calculations of the linear elastic system. This scheme would allow for a complete separation in the accuracy of the geometric model and the accuracy of numerical calculations of the physical system. A local computation scheme can be used to keep the computational complexity linear to the complexity of the physical boundary of the structure, while either first order or higher order approximation methods are available for the space-time discretization.

We have developed a numerical implementation of the

level set method for the structural optimization problem. The benefit and the advantages of the proposed method are illustrated with several 2D examples that have been extensively used in the recent literature of topology optimization, especially in the homogenization based methods.

2 The Optimization Problem

In this paper we use a linear elastic structure to describe the problem of structural optimization. Conceptually, the approach presented here would apply to a general structure model. Let $\Omega \subseteq R^d \quad (d = 2 \text{ or } 3)$ be an open and bounded set occupied by a linear isotropic elastic structure. The boundary of Ω consists of three parts: $\Gamma = \partial\Omega = \Gamma_0 \cup \Gamma_1 \cup \Gamma_2$, with Dirichlet boundary conditions on Γ_1 and Neumann boundary conditions on Γ_2. It is assumed that the boundary segment Γ_0 is traction free. The displacement field u in Ω is the unique solution of the linear elastic system

$$\begin{aligned} -\operatorname{div}\sigma(u) &= f \quad && \text{in} \quad \Omega \\ u &= u_0 && \text{on} \quad \Gamma_1 \\ \sigma(u)\cdot n &= h && \text{on} \quad \Gamma_2 \end{aligned} \tag{1}$$

where the strain tensor ε and the stress tensor σ at any point $x \in \Omega$ are given in the usual form as

$$\varepsilon(u) = \frac{1}{2}\left(\nabla u + \nabla u^T\right) \qquad \sigma(u) = E\varepsilon(u) \tag{2}$$

with E as the elasticity tensor, u_0 the prescribed displacement on Γ_1, f the applied body force, h the boundary traction force applied on Γ_2 such as an external pressure load exerted by a fluid, and n the outward normal to the boundary.

The general problem of structure optimization is specified as

$$\begin{aligned} &\underset{\Omega}{Minimize} \quad Q(u,\Omega) = \int_\Omega F(u)\,d\Omega + \mu|\partial\Omega| \\ &subject\ to: \quad \int_\Omega d\Omega \ \le \ M \end{aligned} \tag{3}$$

where $|\partial\Omega|$ is the Hausdorff measure of the boundary, or perimeter of $\partial\Omega$ and μ is a positive parameter. The inequality describes the limit on the amount of material in terms of the maximum admissible volume M of the design. The variational equation of the linear elastic equilibrium is written as

$$\begin{aligned} &\int_\Omega E\varepsilon(u) : \varepsilon(v)\,d\Omega \\ &\quad = \int_\Omega f\cdot v d\Omega + \int_{\Gamma_2} h\cdot v d\Gamma, \quad \text{for all} \quad v \in U \\ &U = \left\{u : u \in H^1(\Omega);\ u = u_0 \ \text{ on } \ \Gamma_1\right\} \end{aligned} \tag{4}$$

with U denoting the space of kinematically admissible displacement fields and ':' representing the second order tensor operator. The goal of optimization is to find a minimizer Ω for the global criterion $Q(u,\Omega)$ which yields an optimized structure with respect to a specific function described by $F(u)$. This is a standard notion of structural optimization (Bendsoe (1997); Sethian *et al.* (2000)) augmented with the perimeter regularization (Ambrosio *et al.* (1993)).

The design function $F(u)$ may involve any physical or geometric quantity of the design. While the most common choice for $F(u)$ might be the mean compliance of the structure, i.e.,

$$J(u,\Omega) \equiv \int_\Omega F(u)\,d\Omega = \int_\Omega E\varepsilon(u) : \varepsilon(u) d\Omega \tag{5}$$

it may deal with a stress consideration $F(\sigma(u))$ or a displacement function $F(u,x_0) = u(x)\,\delta(x-x_0)$ for $x,\ x_0 \in \Omega$ and $\delta(\cdot)$ being the Dirac delta function.

A fundamental question regarding this class of structural optimization problems (3) is about the existence and smoothness of the solutions. The issue and its significance has been a subject of extensive studies in a class of more general problems of domain identification with regularization (Bourdin *et al.* (2000); Chenais (1975)). For the structural problems of displacement fields satisfying the linear elasticity system, the issue has been investigated in (Ambrosio *et al.* (1993); Bourdin (2000); Larsen (2001)) with some substantial analysis results suggesting that this class of perimeter-regularized problems are well-posed with the existence of smooth solutions. While the mathematical analyses are yet complete, various numerical experiences seem to confirm that the problem formulation provides a well-behaved framework for seeking meaningful optimal solutions, particularly when the models of the structure have finite perimeter. The level set model is indeed such a model as to be presented next.

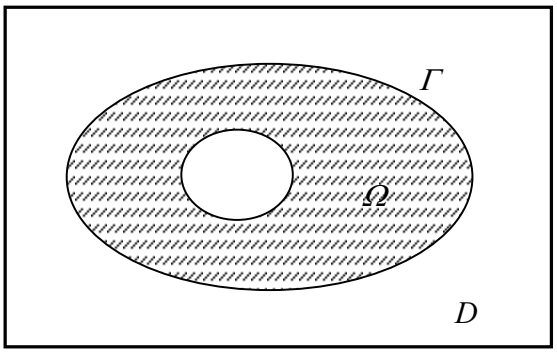

(a). The reference design domain D and the design region Ω.

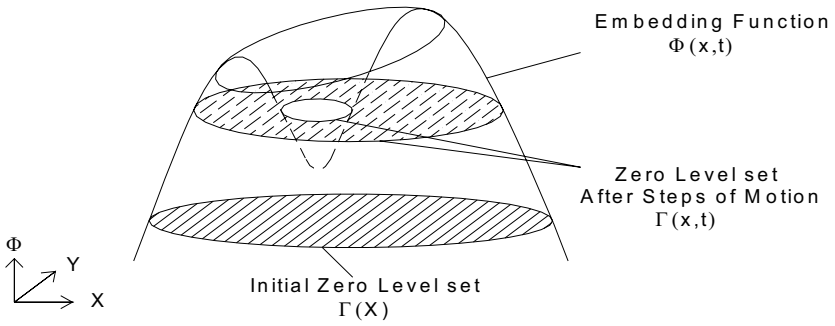

(b). The embedding function $\Phi(x)$ and the level set model Γ.

Figure 1 : The shape boundary, the design region, and the embedding with a level set model.

3 The Level-Set Model of Shape

The level-set method was developed in (Osher *et al.* (2003)) for problems involving the motion of curves and surfaces. It has found many applications (Osher *et al.* (1988); Sethian (1999)) because it allows for automatic changes of topology, such as merging and breaking. One attractive attribute of the method is that it gives a natural way of describing closed boundaries (curves or surfaces) and its calculations can be easily made on a fixed rectilinear grid. With this concept, we can embed the structural boundary surface as the zero level-set of the implicit function, $\Phi : R^d \mapsto R$, such that

$$\Gamma = \{x : \Phi(x) = 0\} \tag{6}$$

The embedding Φ of $(d+1)$ dimension accommodates not only the shape boundary but also the global and regional attribute of the shape, i.e., the shape interior. While the boundary is the zero level-set of the embedding surface, points distant along the shape boundary but close through the interior are connected through the regions of the embedding surface above (or below) the zero level. Thus, the level set is an explicit representation of the solid region of interest by considering the simplest scheme of the following form:

$$\begin{aligned}
&\Phi(x) > 0 \quad \forall x \in \Omega \backslash \partial\Omega \text{ (inside the region)} \\
&\Phi(x) = 0 \quad \forall x \in \partial\Omega \text{ (on the boundary)} \\
&\Phi(x) < 0 \quad \forall x \in D \backslash \Omega \text{ (outside the region)}
\end{aligned} \tag{7}$$

where $D \subset R^d$ is introduced as a fixed design domain which contains all admissible shapes Ω, i.e., $\Omega \subseteq D$, for the convenience of numerical implementation. Therefore, we may refer to the level-set model as a *global* or *region-based* representation (Kimia *et al.* (1995)). These regions of embedding are illustrated in Fig. 1 for a two-dimensional structure. In this case, the boundary curves are embedded in three-dimensional function $\Phi(x)$ with a fixed topology.

The topology optimization can be described as a dynamic

process of level set changing in pseudo-time t. The surface of the embedding function may move up and down on a fixed coordinate system without ever altering its topology. The structural boundary embedded on $\Phi(x)$ can undergo drastic topological changes. However, there is no need to directly track these structural topological changes. The evolution of the implicit function $\Phi(x)$ is obtained by differentiating both sides of (6) with respect to time and by applying the chain rule, yielding the simple Hamilton-Jacobi convection equation

$$\frac{\partial \Phi(x)}{\partial t} + \nabla \Phi(x) \cdot V(x) = 0 \tag{8}$$

where $V(x)$ is the velocity vector of x and it is often referred to as the velocity function of the level-set evolution, i.e.,

$$V(x) = \frac{dx}{dt} \tag{9}$$

Furthermore, by definition of (7), we have $n = -\nabla\Phi/|\nabla\Phi|$ with $|\nabla\Phi| = (\nabla\Phi \cdot \nabla\Phi)^{1/2}$, and $\nabla\Phi \cdot V = -(V \cdot n)|\nabla\Phi|$. Then, equation (8) can be written as

$$\frac{\partial \Phi(x)}{\partial t} = V_n |\nabla \Phi(x)| \qquad V_n = V \cdot n \tag{10}$$

This is known as the *level set equation* (Osher *et al.* (1998, 2003); Sethian (1999)).

Several features and advantages of this method representing the unknown solid shape through the level-set function $\Phi(x)$ become apparent:

1. First, level set models are topologically flexible. The scalar function Φ is defined to always have a simple topology; the representation does not rely on any kind of explicit parameterization. The shape representation is as general as the underlying physical theory. These capabilities would allow the boundary models to easily change the structural topology while undergoing optimization in that they can form holes, split to form multiple boundaries, or merge with other boundaries to form a single surface, in contrast to any conventional boundary shape design (Sethian (1999)).

2. Since the geometric shape is constrained to be the zero level-set of the embedding function $\Phi(x)$, motion of the level set in (10) is permitted only along the normal direction of $\Phi(x)$, driven by the normal velocity $V_n = V \cdot n$. Therefore, the change in the embedded geometric shape is also only in its normal direction. It is well known in differential geometry (Kimia *et al.* (1995); Sapiro (2001)) that for a general velocity vector $V = dx/dt$ its tangential component does not influence the geometry of the shape deformation; it changes only its parameterization. Therefore, the level set equation will not change the parameterization of the solid shape; the level set formulation is a *parameterization free* formulation.

3. In the classical shape optimization theory, there exists an important concept of velocity field of shape deformation (Haug *et al.* (1986); Sokolowski *et al.* (1992)). Based on ideas of continuum mechanics, it has been found that shape derivatives for a diffeomorphism perturbation of a solid exist only in the normal direction of the geometric boundary. The underlying principle of the classical shape optimization is to find a suitable choice of the *normal* velocity field $V_n = V \cdot n$ to ensure a convergent sequence for the optimal solution. Clearly, the level set model provides a natural way to accommodate this requirement. We need to enforce the velocity function V_n in the level set equation to ensure a decrease of the objective functional $Q(u,\Omega)$ such that it is necessary that $V_n(x) = 0$ everywhere on the design boundary Γ at an optimal solution. This will be discussed in detail in next section.

4. Further, a number of numerical techniques have been developed (Osher *et al.* (1998, 2003); Sethian (1999)) to make the initial value problem of (10) computationally robust and efficient. In fact, in the general case of a three dimensional solid structure, the computational complexity can be made proportional to the surface area of the structure rather than the size of its volume. The solutions to the level-set PDE can be accurately computed even when the boundary is not smooth and singularities develop in classical derivatives (Sapiro (2001); Sethian (1999)). This robust property is determined by the unique entropy condition of the Hamilton-Jacobi convection equation (Osher *et al.* (2003)).

With the level set model we can describe the topology optimal problem in terms of the scalar function Φ. It is most convenient to use the Heaviside function H and the Dirac delta function δ defined as

$$H(\Phi) = \begin{cases} 1 & \text{if } \Phi \geq 0 \\ 0 & \text{if } \Phi < 0 \end{cases} \quad \text{and} \quad \delta(\Phi) = \frac{dH}{d\Phi} \tag{11}$$

Therefore, the optimization problem is now written as

follows:

$$\begin{aligned} &\underset{\Phi}{Minimize} \quad Q(u,\Phi) \\ &\qquad = \int_D F(u)\,H(\Phi)\,d\Omega + \mu \int_D \delta(\Phi)\,|\nabla\Phi|\,d\Omega \\ &subject to: \quad g(\Phi) = \int_D H(\Phi)\,d\Omega \;-\; M \le 0 \end{aligned} \tag{12}$$

while the variational equation is written in the energy bilinear and the load linear form as

$$a(u,v,\Phi) \;=\; L(\nu,\Phi) \tag{13}$$

where

$$\begin{aligned} a(u,v,\Phi) \;&=\; \int_D E\varepsilon(u):\varepsilon(v)H(\Phi)d\Omega \\ L(v,\Phi) \;&=\; \int_D (f\cdot v)H(\Phi)d\Omega + \int_D (h\cdot v)\,\delta(\Phi)\,|\nabla\Phi|d\Omega \end{aligned} \tag{14}$$

It is useful to note that

$$|\partial\Omega| = \int_\Gamma d\Gamma = \int_D \delta(\Phi)\,|\nabla\Phi|\,d\Omega$$

4 Shape Derivative and Velocity Field

4.1 Material Derivatives

In the classical shape optimization theory, shape derivative is an important concept as it relates a variation in the shape with the resulting variation in the objective functional. In this case, the design variable is not a function but the direct shape of a geometric domain Ω. (Haug *et al.* (1986); Sokolowski *et al.* (1992)). In order to define the shape derivative, it is convenient to treat Ω. as a continuous medium and to use the material derivative idea of continuum mechanics (Haug *et al.* (1986)). Shape deformation can be viewed as a transformation defined by the mapping $T:\; x \to x_t(x)\,,\; x \in \Omega$, such that

$$x_t = T(x,t) \qquad \Omega_t = T(\Omega,t) \tag{15}$$

This mapping may be regarded as a dynamic process of deforming the shape with pseudo-time t as illustrated in Fig. 2. In a more general method, this transformation can be represented by its velocity

$$V(x_t,t) = \frac{dx_t}{dt}$$

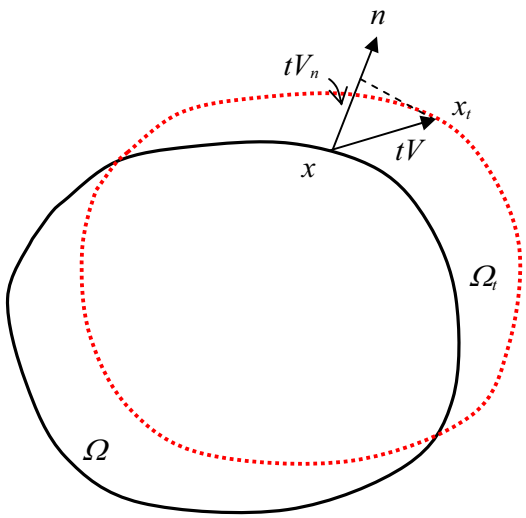

Figure 2 : Shape mapping and variation of shape.

Under sufficient regularity conditions, such as that T^{-1} exists, then the velocity field is given by

$$V(x_t,t) = \frac{\partial T}{\partial t} \circ T^{-1}(x_t,t)$$

Therefore, the shape deformation can be described by the initial-value problem

$$\frac{dx_t}{dt} = V(x_t,t) \qquad x_0 = x \tag{16}$$

This shape deformation analysis leads to the so-called *Lagrangian formulation* of boundary propagation (Sokolowski *et al.* (1992)). When the steady state of this equation is achieved (i.e.,$dx_t/dt = 0$), an optimal shape of the structure is obtained (Haug *et al.* (1986)); Sokolowski *et al.* (1992)). The method has been extensively studied and there are well-established numerical implementations and software systems for boundary shape design (Haug *et al.* (1986)). Unfortunately, this formulation has a sever limitation that only geometry of a *fixed* topology can be handled. In contrast, our level set equation (10) is known as the *Eulerian formulation* of the boundary propagation since the boundary is captured by the implicit function $\Phi(x)$.

Within this context, the shape transformation is defined by the identity

$$x_t = T(x,t) = x + tV(x) \qquad V(x) = V(x,0) \tag{17}$$

This diffeomorphism was introduced by Murat and Simon (see, e.g., (Sokolowski *et al.* (1992)). Thus, a unique velocity field is given as similar to what is defined in the level-set equation (10). Since our global cost $Q(u,\Phi)$ is a functional that depends on the displacement field u and on the shape domain Ω rather than a direct function, we need to use the concept of material derivatives in order to derive the shape derivative of the objective functional (Haug *et al.* (1986)). A comprehensive analysis of the concept has been extensively described in the literature (Haug *et al.* (1986); Sokolowski *et al.* (1992)). We shall utilize three most relevant lemmas that are presented in Appendix. The reader is referred to (Haug *et al.* (1986)) for their proofs.

4.2 Shape Derivative of the Objective Functional

For a given velocity vector V, we now can find the shape derivative of an objective functional. First, we take the material derivative of both sides of the variational equation (14). For the self-adjoint energy bilinear form

$$a(u,v,\Omega)=\int_\Omega E\varepsilon(u):\varepsilon(v)\,d\Omega$$

we obtain the following form, by applying Lemma 1,

$$a'(u,v,\Omega) = \int_\Omega E\varepsilon(\dot{u}):\varepsilon(v)\,d\Omega + \int_\Gamma E\varepsilon(u):\varepsilon(v)(V\cdot n)\,d\Gamma \quad (18)$$

For the load linear form,

$$l(v,\Omega) = \int_\Omega f\cdot v d\Omega + \int_{\Gamma_2} h\cdot v d\Gamma$$

we consider first the conservative loading in which the traction h in (4) depends on position only. Applying Lemma 1 and Lemma 2, it yields the following material derivative

$$l'(v,\Omega) = \int_\Gamma (f\cdot v)(V\cdot n)\,d\Gamma + \int_{\Gamma_2} (\nabla(h\cdot v)\cdot n+\kappa h\cdot v)(V\cdot n)\,d\Gamma \quad (19)$$

We can also consider the more general non-conservative loading case. For example, the traction force of pressure loading in (4) is given as

$$h(x)=-p(x)n(x),\ \ x\in\Gamma_2 \quad (20)$$

Then the material derivative becomes the following, using Lemma 3,

$$l'(v,\Omega) = \int_\Gamma (f\cdot v)(V\cdot n)\,d\Gamma - \int_{\Gamma_2} (\mathrm{div}(pv))(V\cdot n)\,d\Gamma \quad (21)$$

Further, consider our optimization objective functional in the general form

$$J(u,\Omega)\equiv\int_\Omega F(u)\,d\Omega$$

Its Eulerian derivative in the direction of the velocity vector V is obtained by applying Lemma 1, such that,

$$J'(u,\Omega)\equiv dJ(\Omega,V)/dt = \int_\Omega F'(u)\dot{u}d\Omega+\int_\Gamma F(u)(V\cdot n)\,d\Gamma \quad (22)$$

Finally, the general variable formulation gives rise to the following adjoint equation

$$a(\dot{u},v)=\int_\Omega F'(u)\dot{u}d\Omega \quad (23)$$

Thus, equating (18) with (19) and (21) respectively and then using (22) and (23), we obtain the Eulerian derivative of the objective functional, respectively for the conservative traction loading as,

$$J'(u,\Omega) = \int_\Gamma [F(u)+f\cdot v+\kappa h\cdot v+\nabla(h\cdot v)\cdot n-E\varepsilon(u):\varepsilon(v)] (V\cdot n)\,d\Gamma \quad (24)$$

and for the non-conservative loading of pressure traction as,

$$J'(u,\Omega) = \int_\Gamma [F(u)+f\cdot v-\mathrm{div}(pv)-E\varepsilon(u):\varepsilon(v)](V\cdot n)\,d\Gamma \quad (25)$$

Therefore, this derivative can then be expressed in terms of the level set model Φ as

$$J'(u,\Phi)=\int_\Omega \delta(\Phi)G(\Phi)V_n|\nabla\Phi|\,d\Omega \quad (26)$$

where, respectively

$$G(u,v,\Phi) = -(F(u) + (f + \kappa h)\cdot v + \nabla(h\cdot v)\cdot n - E\varepsilon(u):\varepsilon(v))$$

and

$$G(u,v,\Phi) = -(F(u) + f\cdot v - \mathrm{div}(pv) - E\varepsilon(u):\varepsilon(v))$$

In the gradient of the objective functional (26) $G(u,\Omega)$ is known as the *shape gradient density* (Haug *et al.* (1986)). Here, we use the identity that $d\Gamma = \delta(\phi)|\nabla\phi|\,d\Omega$ and the fact that $\Gamma = \{x : \Phi(x) = 0\}$ in changing the boundary integral into the use of the level set geometric representation. Also, $n(\Phi) = -\nabla\Phi/|\nabla\Phi|$ and $\kappa(\Phi) = -\nabla\cdot\left(\nabla\Phi/|\nabla\Phi|\right)$.

It should be particularly noted that the gradient of the objective functional $J(u,\Omega)$ with respect to a shape perturbation with a given velocity vector V is only effective along the normal direction n as specified by the normal velocity component $V_n = V\cdot n$, as illustrated in Fig. 3. Recalling the level set equation (10), the shape boundary represented by the zero level set of the function Φ accommodates its change exactly in the normal direction. Therefore, the level set embedding is complete to represent any shape changes that yield a perturbation of the objective functional.

The gradient of the objective functional may be obtained in a number of different ways. Since the material derivative $\dot{u}$ is linear in V, it is in fact the Fréchet derivative with respect to the shape boundary, evaluated in the direction of V. Thus, one may apply the general Fréchet derivative method for the design gradient as given in (Osher *et al.* (2001); Wang *et al.* (2003)). The use of only the normal component $V_n = V\cdot n$ of the velocity field is justified by the linearity and continuity of the mapping $V \to \dot{u}$ (Haug *et al.* (1986)). Re-parameterization of the shape has no effect on the design objective, and it is cannot be accommodated by the level-set model.

4.3 Steepest Descent Velocity Field

With the above gradient analysis of (26) we can define "naturally" a velocity field $V_n = V\cdot n$ for the level set equation (10) to facilitate an optimization process. In the simplest form of optimization, it amounts to choose a descent direction. The steepest descent direction is directly

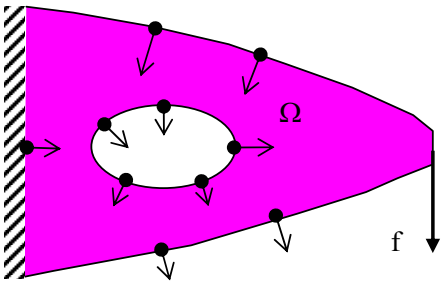

Figure 3 : Normal velocity field in the variation of the shape boundary.

obtained from (25) by setting

$$V_n = -G(\Phi) \quad \text{or} \quad V = -G(\Phi)\,n$$

This particular direction for V is called the *shape gradient*, and it would yield

$$J'(u,\Phi) = -\int_\Omega \delta(\Phi)\,G^2\,|\nabla\Phi|\,d\Omega \le 0 \tag{27}$$

Thus, this choice would give a computational framework for obtaining an approximate solution such as the algorithms used in (Osher *et al.* (2001); Wang *et al.* (2003, 2004)). Theoretical results for the convergence of the steepest descent method are yet known. However, there are now sufficient numerical experiences to support the potential of this formulation (Wang *et al.* (2003, 2004)). In such a numerical implementation, any constraint such as the volume limit is usually incorporated by using a Lagrange multiplier, as detailed in (Osher *et al.* (2001); Wang *et al.* (2003, 2004)).

5 Perimeter Regularization and Geometric Heat Flow

As we have described in the Introduction section the perimeter penalty term $|\partial\Omega|$ introduced in the global criterion of the topology optimization (12) is primarily for the purpose of regularizing the problem to exclude or prevent occurrences of chattering solutions. Further, during the course of shape optimization with the level set models, it is possible that the boundary may not able to maintain certain level of smoothness due to numerical errors of discrete solutions. The boundary may exhibit "fast oscillations". It is highly desirable that the irregularities are removed to enhance the fidelity of the level

sets, while the meaningful discontinuities in the boundary representing topological changes remain to be kept. This is similar to the problem of "denoising" in image processing (Sapiro (2001); Sethian (1999)).

The perimeter regularization used in (12) is essentially defined as a variational problem (Sapiro (2001)). For the boundary perimeter

$$E(\Omega) \equiv |\partial\Omega| = \int_\Gamma d\Gamma = \int_D \delta(\phi)\,|\nabla\phi|\,d\Omega \tag{28}$$

by applying Lemma 2, we have its Eulerian gradient as

$$E'(\Omega) \equiv dE(\Omega)/dt = \int_\Gamma \kappa (V\cdot n)\,d\Gamma$$
$$= \int_\Omega \delta(\Phi)\kappa(\Phi)\,V_n\,|\nabla\Phi|\,d\Omega$$

Again, the steepest descent direction for $E(\Omega)$ can be obtained if we set

$$V_n = V\cdot n = -\kappa \tag{29}$$

and this would yield

$$E'(\Omega) = -\int_\Omega \delta(\Phi)\,\kappa^2\,|\nabla\Phi|\,d\Omega \le 0 \tag{30}$$

Once we introduce this velocity field $V_n = V\cdot n = -\kappa$ into the level set equation (10), we include an important class of shape changes (or deformations) into the process of optimization: *curvature deformation*. It is well known that the curvature deformation corresponds to a parabolic diffusion equation (Kimia *et al.* (1995); Sapiro (2001)). This is also known as the *geometric heat equation* or nonlinear heat equation since the mean curvature $1/(d-1)\kappa$ is a function of time. It represents a global process. In fact, the geometric heat equation would eventually shrink any embedded surface to a circular point (Sapiro (2001)). This property serves as a strong means to prevent any microscopic holes from existing in the process of optimization, thus making the problem well-posed. In addition, the geometric heat deformation has a remarkable smoothing effect: it decreases the local maxima of κ while increases its local minima. Thus, large oscillations are immediately smoothed out, and a long term solution results from dissipation of information about the initial state of $\partial\Omega$ (Sapiro (2001); Sethian (1999)). More importantly, this mean curvature flow is an anisotropic diffusion (Wang and Zhou (2004)), unlike a linear heat equation of the Gaussian filtering (Bourdin (2001)). The geometric boundary gets diffused only in the tangential direction of the surface, and there is no "side-effect" of "averaging". Therefore, the regularization term of (27) plays a role in fairing the level sets only without any effect on their normal motion. This property can also be explained from the point of view of the so-called total variation energy (Osher *et al.* (1988); Sapiro (2001)), since the perimeter regularization has the identical result as reducing the total variation of the boundary. The advantages of anisotropic smoothing have been widely exploited in imaging processing (Sapiro (2001)), i.e., in edge detection and image segmentation.

In a perspective of nonlinear heat equations, there might be other successful regularization strategies rather than the perimeter measure, such as affine geometric heat flow $\left(V_n = -\kappa^{1/3}\right)$ and constant velocity flow $(V_n = -1)$. In the level-set framework, a heat equation is naturally accommodated for geometric singularities defined by topology changes. Based on the theory of viscosity solutions, the level set equation allows for extensions of flows such as the geometric heat flow to non-smooth curves and surfaces, as to be discussed in the next section.

6 Numerical Computations

Now, we can combine the Eulerian gradients of the objective functional (27) and the perimeter penalty (30) to obtain the velocity field for minimizing the global criterion $G(u,\Omega)$ (12), expressed in terms of the level set model, as follows

$$V_n(u,w,\Phi) = -G(u,w,\Phi) - \mu\kappa(\Phi) \tag{31}$$

Therefore, by substituting (31) into the level set equation (10), we need to solve a final PDE to obtain the steepest descent solution for an optimal solution of $Q(u,\Omega)$:

$$\frac{\partial\Phi(x)}{\partial t} - [G(\Phi) + \mu\kappa(\Phi)]\,|\nabla\Phi(x)| = 0 \tag{32}$$

There are a number of computational issues that are important to the proposed level set method. First, the level set embedding is defined at the particular zero level $\Phi(x,t) = 0$. This fact can be exploited to develop highly efficient algorithms which reduce the computational complexity to the physical level of the structural (Osher *et al.* (1988); Sethian (1999)). Second, a set of highly accurate and robust numerical algorithms have

been developed for a discrete solution of the PDE of (10) (Osher *et al.* (1988, 2003); Peng *et al.* (1999)). Third, an approximate solution to the system equation of the linear elasticity is usually obtained with a finite element method. In this section, we discuss a numerical implementation of the level set method with a structure finite element mesh and a rectilinear spatial grid. Some key aspects of the implementation are described here, while other details related to the standard level set calculus are referred to (Sethian, (1999)).

6.1 Numerical and Finite Element Approximation

Numerical approximation for the level set equation (32) can be easily implemented using the standard approach of discretizing $x - t$ space into a collection of grid points with $\Delta x = h_x$ and $\Delta t = h_t$. For convenience, usually a rectilinear grid for $x \in R^d$ is used.

In general, the linear elastic equation (4) may be solved by using a finite element method. For the purpose, one may chose to use an adaptive meshing scheme with a more explicit description of the boundary as discussed in (Bourdin *et al.* (2000)). Such an implementation is typically complicated. Another technique is to use a fixed, structured mesh, as it is often seen in homogenization-based topology optimization (Bendsoe (1997); Bendsoe *et al.* (1988); Haber *et al.* (1996)). This has an added advantage that a fixed, rectilinear grid for the numerical approximation of the level set PDE can be made coincidental to some nodes of a rectilinear finite element mesh, rendering a more straightforward numerical implementation.

Based on this idea, the permissible design space $D \subseteq R^d$ is first specified for the given problem, in a similar manner that the "ground structure" is specified in a homogenization-based approach (Bendsoe (1997)). Proper boundary conditions are specified on ∂D such as Neumann conditions and Dirichlet conditions as shown in Fig. 4. The reference space D is then discretized with a rectilinear mesh for a specific spatial interval $\Delta x = h_x$, $1/2h_x$, or coarser (finer). Note that the resolution of spatial grid $\Delta x = h_x$ is essentially determined based on the numerical accuracy required for an approximated solution of the level set PDE (32), while the resolution of the finite elements determines the accuracy of the approximation of the linear elastic equation (4). This accuracy can also be improved by using a high order interpolation scheme in finite element calculations (i.e., using p-version elements). In contrast to a homogenization-based method with a "raster geometry" model, the accuracy of geometric representation is entirely separated with the accuracy of the finite element solution of the system mechanics. For example, if the design objective is only the mean compliance of the structure, the accuracy of its approximation is not nearly as important as that of the Hamilton-Jacobi equation. In that case, we may select a finite element mesh coarser than the rectilinear grid without any major compromise of the accuracy of the final numerical solution.

In the process of level-set based optimization, the design represented by the level-set model is initialized as Ω_0 at $t = 0$ such that its boundary fully contains that of D, $\partial D \subseteq \partial\Omega_0$. As the optimization proceeds, the geometric boundary $\partial\Omega$ will be changed as motion defined by the level-set partial differential equation (10) until a termination as illustrated in Fig. 4. At a successful optimization, the final optimal shape Ω will be a subset of the fixed reference domain, $\Omega \subseteq D$, as required by the optimality conditions and the constraints.

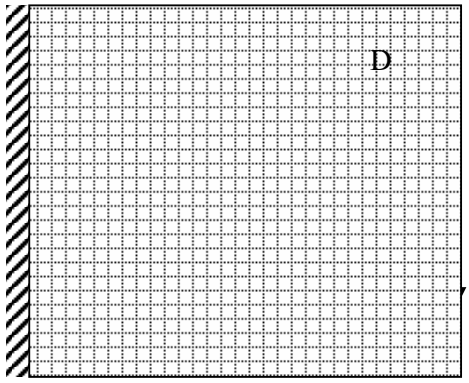

Figure 4 : Finite elements of a rectilinear grid in the fixed reference domain D and the solid shape embedded by the level set model Ω. The boundary condition on Γ_1 is specified on the fixed reference domain D.

Since the finite elements are fixed during the optimization procedure, we must ensure that the structural system is non-singular. This can be dealt with by the classical assumption that the set $D\backslash\Omega$ is filled with a "fictitious material" of small mass density $\rho/\rho_0 = \varepsilon_\rho$, where ρ_0 represents the mass density of the homogeneous material.

Therefore,

$$\rho(\Phi) = \rho_0[(1-\varepsilon_\rho) H(\Phi) + \varepsilon_\rho] \tag{33}$$

Further, in the numerical implementation, functions $\delta(\Phi)$ and $H(\Phi)$ have to be approximated with a first order accurate, smoothed version such as defined in (Osher *et al.* (1988, 2001)). Thus, we define the following approximation functions (Wang *et al.* (2003))

$$H(\Phi) = \begin{cases} 0 & \Phi < -\xi \\ \frac{3}{4}\left(\frac{\Phi}{\xi} - \frac{\Phi^3}{3\xi^3}\right) + \frac{1}{2} & -\xi \le \Phi < \xi \\ 1 & \Phi \ge \xi \end{cases}$$
$$\delta(\Phi) = dH(\Phi)/d\Phi \tag{34}$$

where ξ is a parameter of choice to determine the size of the bandwidth of numerical smoothing.

In this fashion, the geometric boundary of the structure under optimization is always implicitly described as the zero level set of $\Phi(x,t) = 0$. There is no need to explicitly recover the boundary until the end of the optimization (Wang *et al.* (2003)). There exist many techniques in most of the popular scientific software systems to compute iso-curves and iso-surfaces. For example, the well-known marching-cubes technique in computer graphics can be directly applied to recover 2D and 3D level sets.

6.2 Discrete Computation Schemes

The discrete solution to the Hamilton-Jacobi equation (10) is computed using finite differences over discrete time steps $\Delta t = h_t$ and on the discrete grid $\Delta x = h_x$ over the level set function. A highly robust and accurate computational method was developed by Osher and Sethian (1988) to address the problem of overshooting. Based on the notion of weak solutions and entropy limits, a so called "up-wind scheme" is proposed to solve (10) with the following first order update equation

$$\phi_{ijk}^{n+1} = \phi_{ijk}^{n} - \Delta t \left(\max\left((V_n)_{ijk}, 0\right)\nabla^+ + \min\left((V_n)_{ijk}, 0\right)\nabla^-\right) \tag{35}$$

where

$$\nabla^+ = \{\max(D_{ijk}^{-x},0)^2 + \min(D_{ijk}^{+x},0)^2 + \max(D_{ijk}^{-y},0)^2 + \min(D_{ijk}^{+y},0)^2 + \max(D_{ijk}^{-z},0)^2 + \min(D_{ijk}^{+z},0)^2\}^{1/2},$$

$$\nabla^- = \{\max(D_{ijk}^{+x},0)^2 + \min(D_{ijk}^{-x},0)^2 + \max(D_{ijk}^{+y},0)^2 + \min(D_{ijk}^{-y},0)^2 + \max(D_{ijk}^{+z},0)^2 + \min(D_{ijk}^{-z},0)^2\}^{1/2}$$

and, Δt is the time step, and $D_{ijk}^{\pm x}, D_{ijk}^{\pm y}$ and $D_{ijk}^{\pm z}$ are the respective forward $(+)$ and backward $(-)$ difference operators on Φ_{ijk}^n in the three dimensions of $x \in R^3$ separately. In addition, the time steps Δt must be limited to ensure the stability of the up-wind scheme (35). The Courant-Friedrichs-Lewy (CFL) condition requires Δt to satisfy

$$\Delta t \max \left|(V_n)_{ijk}\right| \le \Delta_{\min} \quad \Delta_{\min} = \min(\Delta x, \Delta y, \Delta z) \tag{36}$$

where $\Delta_{\min}$ stands for the minimum grid space among the three spatial dimensions (Osher *et al.* (2003)).

Higher order schemes can also be obtained for the space quantities ∇^+ and ∇^- for discrete approximation. They are typically constructed with an essentially non-oscillatory (ENO) interpolation as fully described in (Shu *et al.* (1988)). We have implemented this so-called "high resolution" scheme and fount that it is indeed more accurate than the first order scheme (Wang *et al.* (2003)). The first order time-explicit scheme (35) is well known for its numerical stability. It can be made of higher order through a total variation diminishing (TVD) Runge-Kutta scheme (Shu (1988)). As outlined in the literature (Sethian (1999); Shu (1988); Wang *et al.* (2003)), these schemes are explicit schemes and hence can be implemented in a straightforward manner.

6.3 Local Schemes of Level Set Computation

While the up-wind scheme makes the level set method numerically robust, the level set equation can also be made with its computational complexity proportional to the boundary area of the structure being optimized rather than the size of the volume in which it is embedded. This is because the structural boundary is defined to be a single level set (at the zero level), thus the calculation of solutions over the entire range of the function Φ is unnecessary.

An efficient method has been developed in (Peng *et al.* (1999)) by making the embedding function Φ as a distance function. Then, while the function Φ is maintained to be a signed distance function, a local computation of the level set requires update only those points where $\Phi \approx 0$. This *local computation scheme* is simple and efficient. It has been shown that this method has a formal complexity of $O(N)$ in the 2D case and $O(N^2)$ in the 3D solid case, where N is the size of the spatial grid in each direction of the level set (Peng *et al.* (1999)). In other words, the complexity of the level set model computation remains at the level of its physical dimension, not of the higher dimension of its embedding function. This advantage makes the local level set method practically attracting.

In this scheme we compute the signed distance function as defined as the Eikonal equation

$$|\nabla\Phi(x,t)| = 1 \tag{37}$$

This gives rise to another PDE to solve for its steady state,

$$\frac{\partial\Phi}{\partial t} = \text{sign}(\Phi)(1-|\nabla\Phi|) \tag{38}$$

where $\text{sign}(\Phi) = 2H(\Phi) - 1$ is the signed distance function (Osher *et al.* (1988)). This approach allows us to avoid finding the design boundary explicitly. Furthermore, it also serves a purpose of re-initialization of the level set function $\Phi(x,t)$ in order to obtain highly accurate numerical results (Osher *et al.* (1988)). The solution of this PDE would prevent $\Phi(x,t)$ from deviating away from the signed distance function.

6.4 Velocity Extension and Smoothing

In the level set formulation, we need the normal velocity V_n in a neighborhood of the design boundary or the zero level set $\Gamma(t)$. As suggested in (Sethian (1999)), the most natural way to extend V_n off the design boundary is to let the velocity V_n be constant along the normal to $\Gamma(t)$ such that

$$\nabla V_n \cdot \nabla\Phi = 0 \tag{39}$$

This leads to the following hyperbolic partial differential equation

$$\frac{\partial V_n}{\partial t} + sign(\Phi)\frac{\nabla\Phi}{|\nabla\Phi|}\cdot\nabla V_n = 0 \tag{40}$$

Accurate and robust numerical schemes, such as the first order upwind method, exist to compute discrete solutions to partial differential equations of velocity extension (Sethian (1999)). For simplicity of the presentation, the reader is referred to (Osher *et al.* (1988); Peng *et al.* (1999)) for detailed formulae.

As a notable advantage of the level set method, the structural boundary is not tracked explicitly while the level set equation is solved over the rectilinear grids. Therefore, the velocity field defining the level set movement cannot be directly evaluated for the boundary surface. We use a smoothing method to evaluate the velocity field over the finite element nodes. We may introduce a general and positive function with tight support as a weighting function, such as the Gaussian function

$$\alpha(x) = \frac{1}{\sqrt{2\pi}\Delta_{\min}} e^{-\Phi^2(x)/\Delta^2_{\min}} \tag{41}$$

with a constant $\Delta_{\min}$ representing the minimal width of the along the level sets. The purpose is to use it to smooth the velocity vector V_n with an effect on the gradient of the objective functional such that

$$\min_{\tilde{V}_n} \int_D \left(\alpha(x)\tilde{V}_n(\Phi) - V_n(u,w,\Phi)\,\delta(\Phi)\right)^2 d\Omega \tag{42}$$

By solving this least squares smoothing equation, we obtain a new non-local velocity field $\tilde{V}_n(\Phi)$ defined on the rectilinear grid of computation.

7 Numerical Examples

Numerical examples are presented in this section for mean compliance optimization problems that have been widely studied in the relevant literature (Bendsoe (1997); Bulman *et al.* (2001)). The objective function of the problem is the strain energy of the structure with a material volume constraint,

$$J(u,\Omega) = \int_D E\varepsilon(u) : \varepsilon(u) d\Omega \tag{43}$$

For all examples, the material used is steel with a modulus of elasticity of 200 GPa and a Poisson's ratio of ν= 0.3. For clarity in presentation, the examples are in 2D under plane stress condition.

7.1 MBB Beams

This example is known as MBB beams related to a problem of designing a floor panel of a passenger airplane in

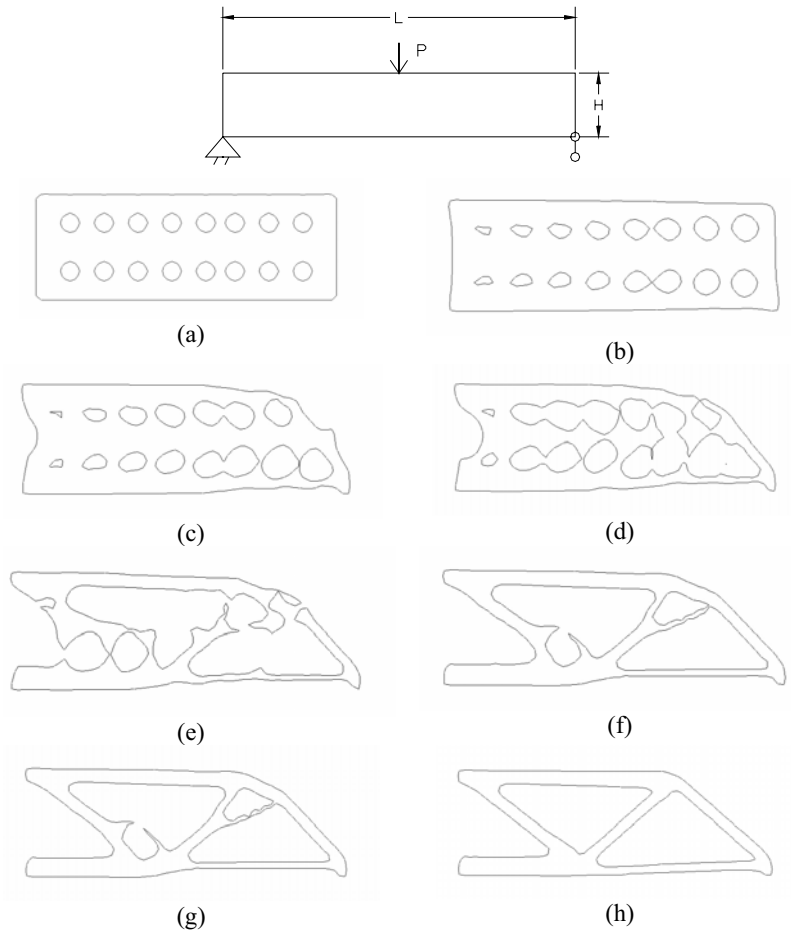

Figure 5 : A mid-point loaded MBB beam with fixed-simple supports and a volume ratio of 0.3. (a) Initial design of the right half. (b – g) Intermediate results. (h) Final solution.

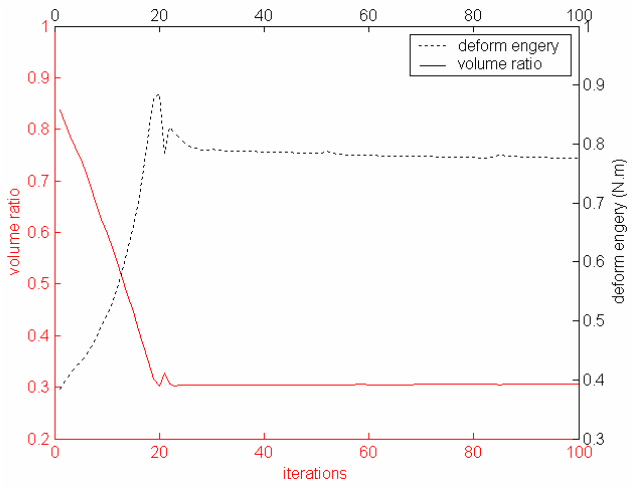

Figure 6 : The mean compliance and the volume of the structure over iteration for example of Fig. 5.

Germany. The floor panel is loaded with a concentrated vertical force $P = 80N$ at the center of the top edge. It is has a fixed support and a simple support at its bottom corners respectively. The design domain has a length to height ratio of 12:2.

In Fig. 5 the volume ratio is specified to be 0.3, and we use 22×62 quadrilateral elements to model a half of the structure due to the geometric symmetry. The numerical width ξ of the Heaviside function is taken the same with the grid width. The changes of the objective function and the structure volume over the iteration are shown in Fig. 6. In Fig. 7 the volume ratio is specified to be 0.35, and 56×156 quadrilateral elements are used. The numerical width ξ of the Heaviside function is taken as 0.8 times of the grid width. The changes of the objective function and the structure volume over the iteration are shown in Fig. 8. In Fig. 9 the volume ratio is increased to 0.355, while

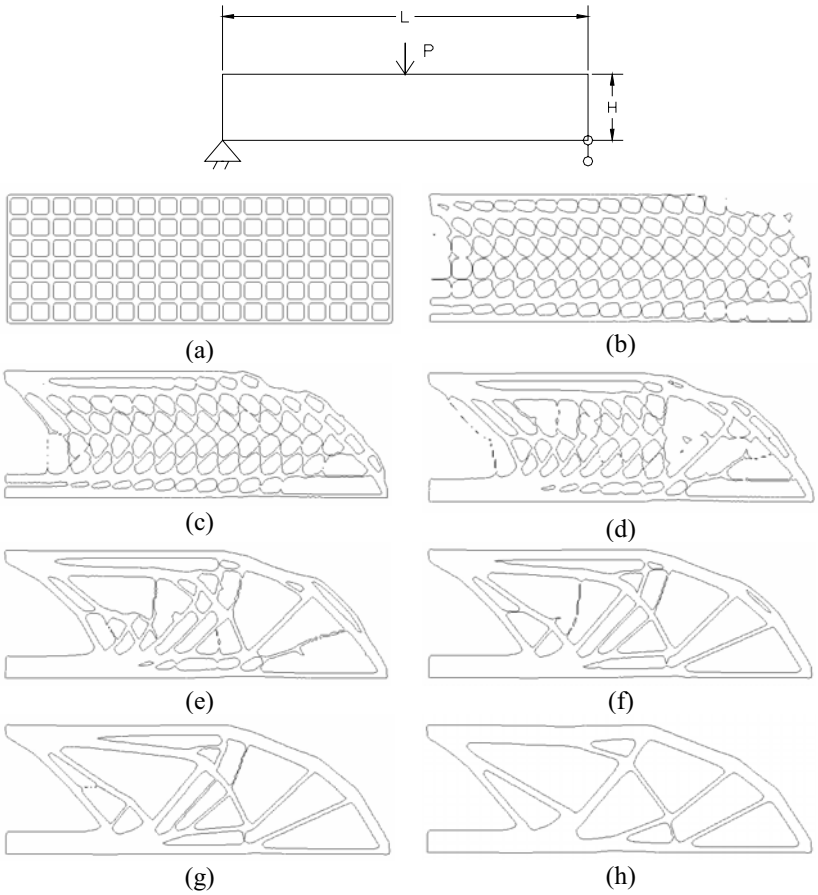

Figure 7 : A mid-point loaded MBB beam with a volume ratio of 0.35. (a) Initial design of the right half. (b – g) Intermediate results. (h) Final solution.

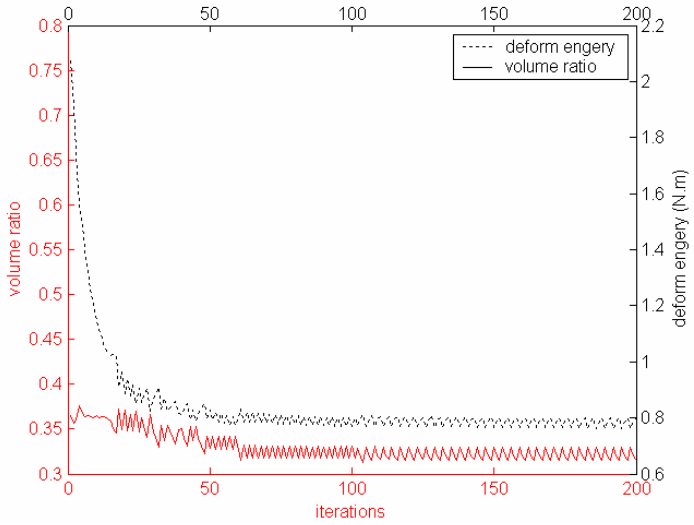

Figure 8 : The mean compliance and the volume of the structure over iteration for example of Fig. 7.

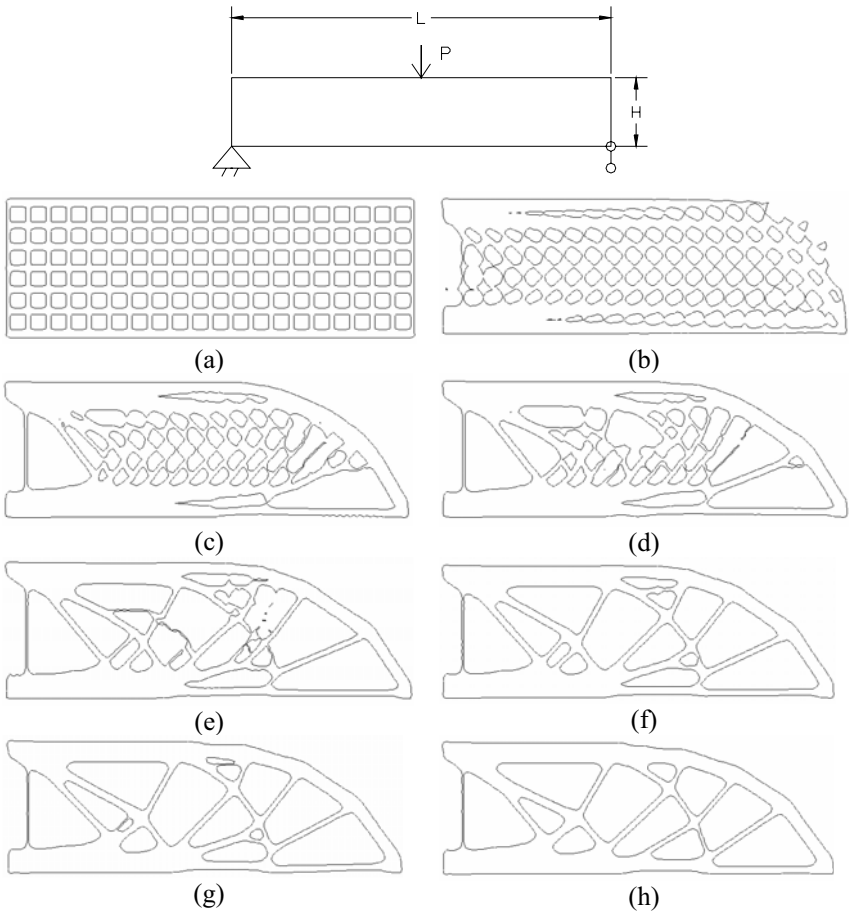

Figure 9 : A mid-point loaded MBB beam with a volume ratio of 0.355. (a) Initial half design. (b – g) Intermediate results. (h) Final solution.

ξ is taken as 0.5 times of the grid width. The changes of the mean compliance and the volume over the iteration are shown in Fig. 10.

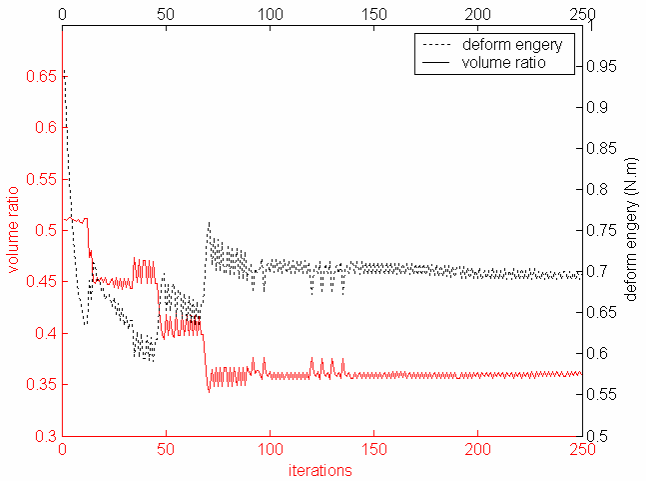

Figure 10 : The mean compliance and the volume of the structure over iteration for example of Fig. 9.

7.2 Cantilever Beam

The second example is a cantilever beam with a concentrated vertical force $P = 80N$ at the bottom of its free vertical edge. The design domain has a length to height ratio of 3.2:2. In Fig. 11 the volume ratio is specified to be 0.3, and we use 22×34 quadrilateral. The numerical width ξ of the Heaviside function is taken the same with the grid width. The changes of the mean compliance and the structure volume over the iteration are shown in Fig. 12.

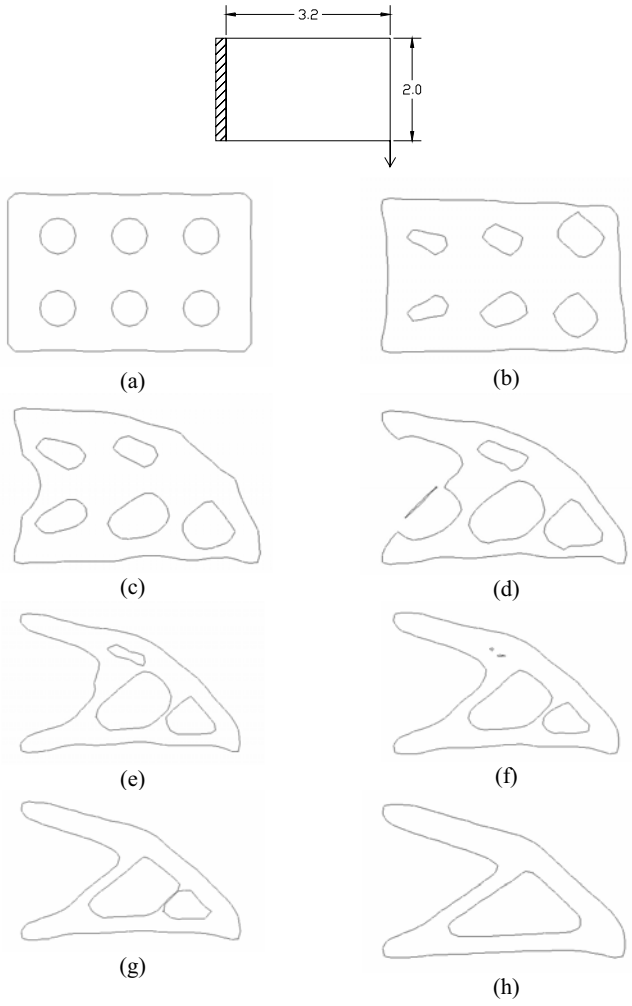

Figure 11 : A cantilever beam with volume ratio of 0.3. (a) Initial design. (b – g) Intermediate results. (h) Final solution.

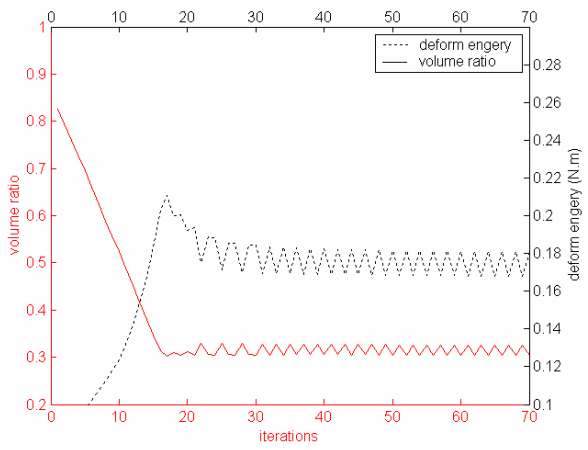

Figure 12 : The mean compliance and the volume of the structure over iteration for example of Fig. 11.

7.3 Bridge Structures

A bridge type structure is considered next. A rectangular design domain of L long and H high with a ratio of $L : H = 12 : 6$ is loaded vertically at the center point of its bottom with $P = 30N$ as shown in Fig. 13. The left bottom corner of the beam is fixed, while it is simply supported at the right bottom corner. The volume ratio of 0.31 is considered. The initial design and some intermediate and the final optimization results are shown in Fig. 13. The final optimum solution is nearly identical to what other researchers have obtained using a homogenization based method (Bendsoe (1997); Bulman *et al.* (2001)). A mesh of 62×122 quadrilateral elements are used for the finite element analysis, and the numerical width ξ for the approximate Heaviside function is chosen to be 0.7

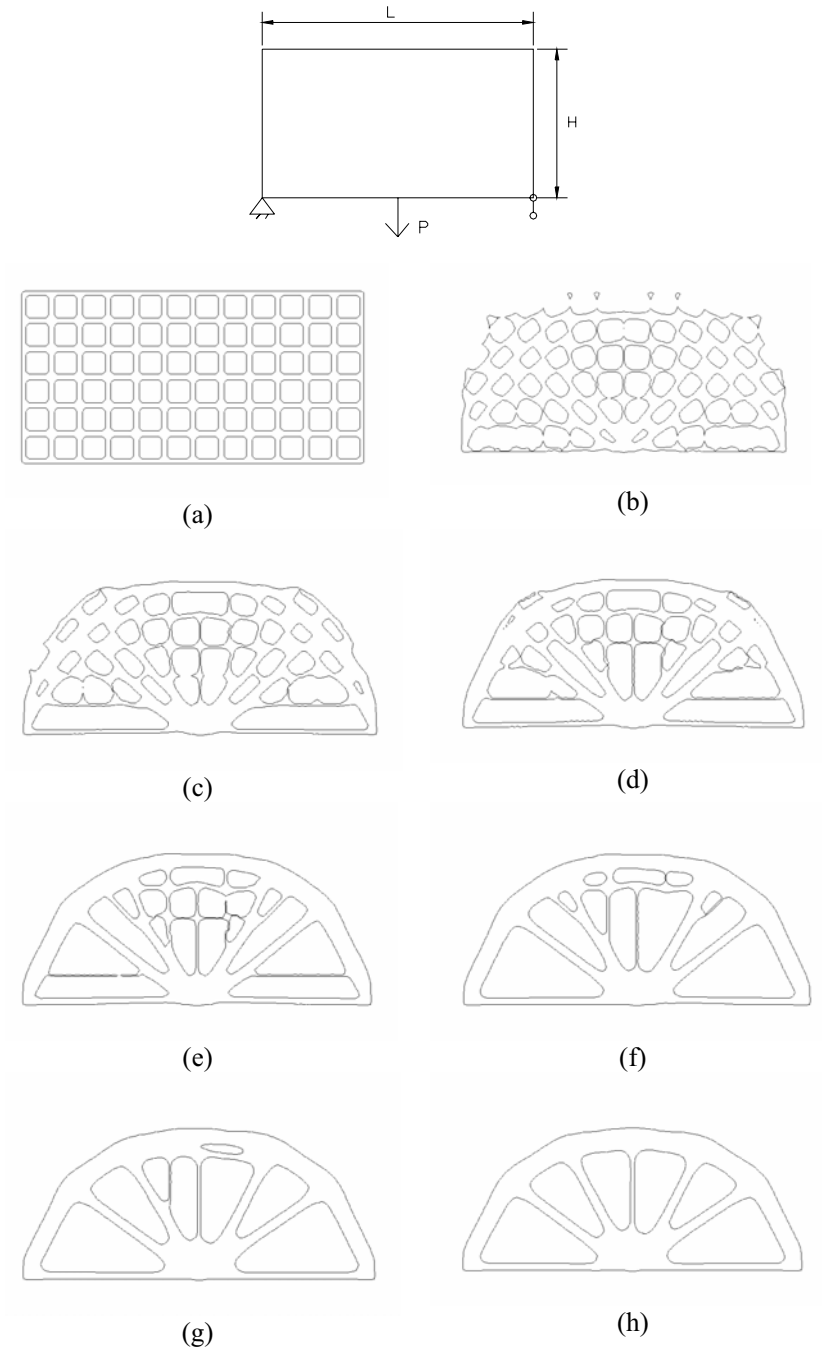

Figure 13 : A bridge type structure with fixed-simple supports. (a) Initial design. (b – g) Intermediate results. (h) Final solution.

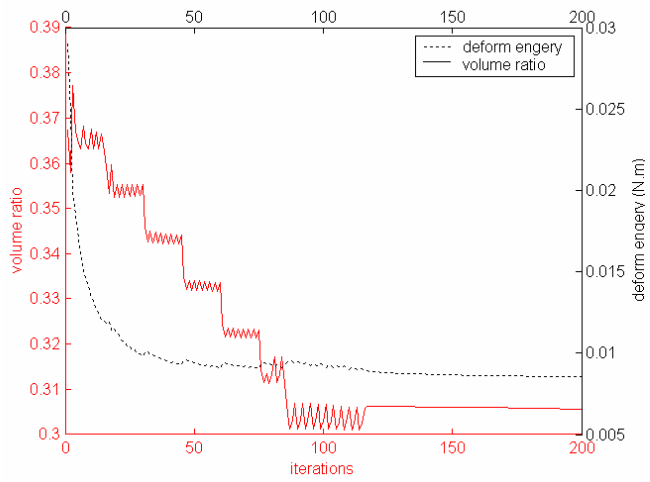

Figure 14 : The mean compliance and the volume of the structure over iteration for example of Fig. 13.

times of the grid width.

Another bridge type structure is considered with multiple loads at its bottom as shown in Fig. 15, with $P_1 = 40N$ and $P_2 = 20N$. Again the volume ratio is 0.3. The initial design and some intermediate and the final optimization results are shown. Changes in the mean compliance and the body volume during the iterations of optimization are shown in Fig. 16.

8 Conclusions

We have presented a level-set based method for structural shape and topology optimization. We have shown that the level set representation is in fact a *region representation* of the structure's shape with the capability to provide an extra "dimension" of information by allowing for changes of the three-dimensional boundary in a higher four-dimensional space constrained to embed the original problem. This model leads naturally to a dynamic framework of a Hamilton-Jacobi partial differential equation governing permissible motions of the level sets with flexibility of handling topological changes. We have established a relationship between the velocity field in the Hamilton-Jacobi equation to the shape derivative of the classical shape variation. This relationship justifies a proper choice of the velocity field for an optimization process. We have studied the effect of a Hausdorff measure (perimeter) penalty. Fundamentally, a perimeter penalization restricts the feasible design space to eliminate chattering solutions and thus ensures the existence of smooth solutions. At the same time, the regularization adds curvature diffusion to the optimization process. This leads to a desirable effect of an anisotropic filtering to smooth the geometric boundary without any "damage" on the convergence of the optimization process. We further described numerical techniques for efficient and robust implementation of the proposed method, by embedding a rectilinear grid in a fixed finite element mesh defined on a reference design domain. This would separate the accuracy issues of numerical calculations of the physical equation and the evolution of the level-set model. The benefit and the advantages of the developed method are illustrated with several 2D examples that have been extensively used in the recent literature of topology optimization, especially in the homogenization based methods.

In our numerical implementation, we have used the second order approximations of the TVD Runge-Kutta scheme and the ENO "upwind" scheme for discrete space-time solutions. While this implementation gives rise to accurate and stable numerical solution as predicted, we have noticed that the convergence speed of the method could be improved. A promising technique is to incorporate a nonlinear velocity mapping. It has been shown in (Wang *et al.* (2004)) to be able to substantially increase the computational efficiency from the basic gradient descent method.

While we demonstrated the method only with examples of mean compliance optimization in two dimensions, this is mainly for convenience. The approach adopted here naturally lends itself to more general optimal design

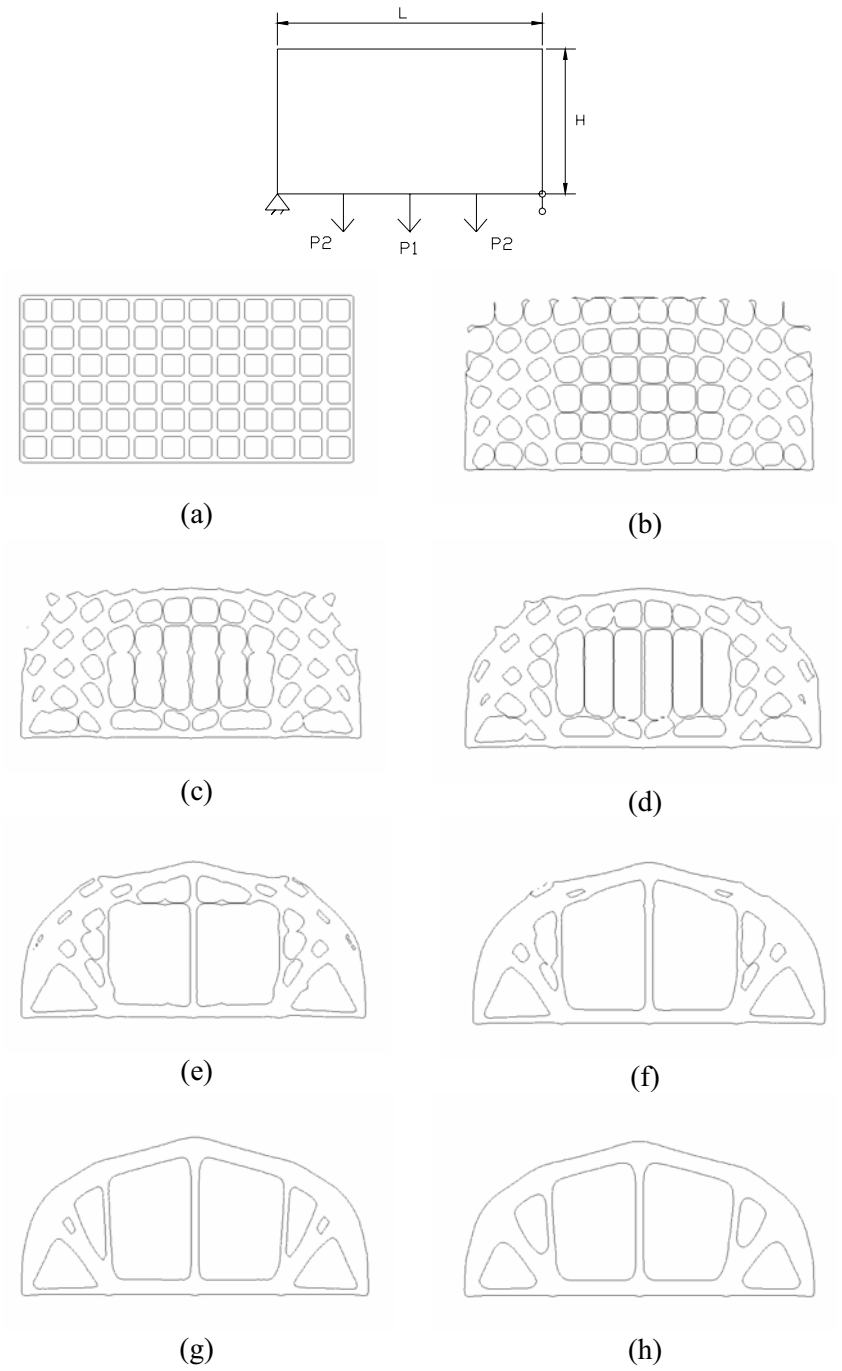

Figure 15 : A bridge type structure with multiple loads. (a) Initial design. (b – g) Intermediate results. (h) Final solution.

problems involving multi-physics and/or multi-domains. In fact, we have extended the approach to a multi-phase model of level set for problems of optimization of heterogeneous materials and/or graded materials. The results are to be reported separately.

Acknowledgement: This research work is supported in part by the Research Grants Council of Hong Kong SAR (Project No. CUHK4164/03E) and the Natural Science Foundation of China (NSFC) (Grants Nos. 50128503, 50305019, and 50390063).

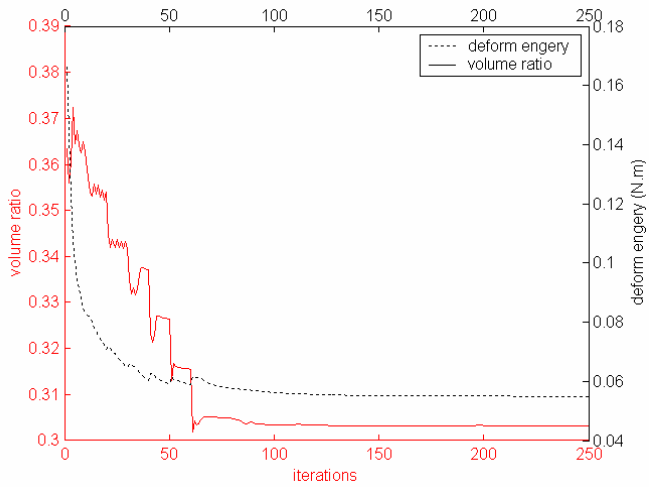

Figure 16 : The mean compliance and the volume of the structure over iteration for example of Fig. 15.

References

Allaire, G.; Jouve, F.; Taoder, A.-M. (2002): A level-set method for shape optimization. *C. R. Acad. Sci. Paris, Ser. I*, vol. 334, pp. 1125-1130.

Ambrosio, L.; Buttazzo, G. (1993): An optimal design problem with perimeter penalization. *Calculus of Variations and Partial Differential Equations*, vol. 1, pp. 55-59.

Bendsoe, M. P. (1989): Optimal shape design as a material distribution problem. *Structural Optimization*, vol. 1, pp. 193-202.

Bendsoe, M. P. (1997): Optimization of Structural Topology, Shape and Material, Springer, Berlin.

Bendsoe, M. P.; Haber, R. (1993): The Michell layout problem as a low volume fraction limit of the homogenization method for topology design: An asymptotic study. *Structural Optimization*, vol. 6, pp. 63-267.

Bendsoe, M. P.; Kikuchi, N. (1988): Generating optimal topologies in structural design using a homogenisation method. *Computer Methods in Applied Mechanics and Engineering*, vol. 71, pp. 197-224.

Bendsoe, M. P.; Sigmund, O. (1999): Material interpolations in topology optimization. *Archive of Applied Mechanics*, vol. 69, pp. 635-654.

Bourdin, B. (2001): Filters in topology optimization. *International Journal for Numerical Methods in Engineering*, vol. 50, pp. 2143-2158.

Bourdin, B.; Chambolle, A. (2000): Implementation of an adaptive finite-element approximation of the Mumford-Shah functional. *Numer. Mathemat*, vol. 85(4), pp. 609-646.

Bulman, S.; Sienz, J.; Hinton, E. (2001): Comparisons between algorithms for structural topology optimization using a series of benchmark studies. *Computers and Structures*, vol. 79, pp. 1203-1218.

Chenais, D. (1975): On the existence of a solution in a domain identification problem. *Journal of Mathematical Analysis and Application*, vol. 52(2), pp. 189-219.

Cheng, K.-T.; Olhoff, N. (1981): An investigation concerning optimal design of solid elastic plates. *International Journal of Solids and Structures*, vol. 17, pp. 305-323.

Diaz, R.; Bendsoe, M. P. (1992): Shape optimization of structures for multiple loading conditions using a homogenization method. *Structural Optimization*, vol. 4, pp. 17-22.

Diaz, R.; Sigmund, O. (1995): Checkerboards patterns in layout optimization. *Structural Optimization*, vol. 10, pp. 10-45.

Haber, R. B.; Jog, C. S.; Bendsoe, M. P. (1996): A new approach to variable-topology shape design using a constraint on perimeter. *Structural Optimization*, vol. 11, pp. 1-12.

Haug, E. J.; Choi, K. K.; Komkov, V. (1986): Design Sensitivity Analysis of Structural Systems, Academic Press, Orlando.

Kimia, B. B.; Tannenbaum, A. R.; Zucker, S. W.

(1995): Shape, shock, and deformations I: the components of two-dimensional shape and reaction-diffusion space. *International Journal of Computer Vision*, vol. 15, pp. 189-224.

Larsen, J. (2001): Regularity in two-dimensional variational problems with perimeter penalties. *C. R. Acad. Sci. Paris Ser. I Math.*, vol. 333(3), pp. 261-266.

Lin, C.Y.; Chao, L.-S. (1992): Automated image interpretation for integrated topology and shape optimization. *Structural and Multidisciplinary Optimization*, vol. 20, pp. 124-137.

Mlejnek, H. P. (1992): Some aspects of the genesis of structures. *Structural Optimization*, vol. 5, pp. 64-69.

Osher, S.; Sethian, J. A. (2003): Front propagating with curvature-dependent speed: Algorithms based on Hamilton-Jacobi formulations. *Journal of Computational Physics*, vol. 79, pp. 12-49.

Osher, S.; Fedkiw, R. (2003): Level Set Methods and Dynamic Implicit Surfaces, Springer, New York.

Osher, S. J.; Santosa, F. (2001): Level set methods for optimization problems involving geometry and constrains I. Frequencies of a two-density inhomogeneous drum. *Journal of Computational Physics*, vol. 171, pp. 272-288.

Peng, D. *et al.* (1999): A PED-based fast local level set method, *Journal of Computational Physics*, vol. 155, pp. 410-438.

Petersson, J. (1999): Some convergence results in perimeter-controlled topology optimization. *Computer Methods in Applied Mechanics and Engineering*, vol. 171, pp. 123-140.

Petersson, J.; Sigmund, O. (1998): Slope constrained topology optimization, *International Journal for Numerical Methods in Engineering*, vol. 41, pp. 1417-1434.

Rozvany, G. (1988): Structural Design via Optimality Criteria, Kluwer, Dordrecht.

Rozvany, G. (2001): Aims, scope, methods, history and unified terminology of computer aided topology optimization in structural mechanics. *Structural and Multidisciplinary Optimization*, vol. 21, pp. 90-108.

Sapiro, G. (2001): Geometric Partial Differential Equations and Image Analysis, Cambridge University Press, Cambridge.

Sethian, J. A.; Wiegmann, A. (2000): Structural boundary design via level set and immersed interface methods. *Journal of Computational Physics*, vol. 163(2), pp. 489-528.

Sethian, J. A. (1999): Level Set Methods and Fast Marching Methods: Evolving Interfaces in Computational Geometry, Fluid Mechanics, Computer Vision, and Materials Science, Cambridge University Press.

Sheen, D.; Seo, S.; Cho, J. (2003): A level set approach to optimal homogenized coefficients. *CMES: Computer Modeling in Engineering & Sciences* Vol. 4, No. 1, pp. 21-30.

Shu, C.-W. (1988): Total-variation-diminishing time discretization. *SIAM J. Sci. Stat. Comput*, vol. 9, pp. 1073-1084.

Shu, C.-W.; Osher, S. (1988): Efficient implementation of essentially non-oscillatory shock capture schemes. *Journal of Computational Physics*, vol. 77, pp. 439-471.

Sigmund, O. (2000): Topology optimization: A tool for the tailoring of structures and materials. *Phil. Trans.: Math. Phys. Eng. Sci.*, vol. 358, pp. 211-228.

Sigmund, O. (2001): A 99 topology optimization code written in Matlab. *Structural and Multidisciplinary Optimization*, vol. 21, pp. 120-718.

Sigmund, O.; Petersson, J. (1998): Numerical instabilities in topology optimization: a survey on procedures dealing with checkerboards, mesh-dependencies and local minima, *Structural Optimization*, vol. 16(1), pp. 68-75.

Sokolowski, J.; Zolesio, J. P. (1992): Introduction to Shape Optimization: Shape Sensitivity Analysis, Springer-Verlag, New York.

Suzuki, K.; Kikuchi, N. (1991): A homogenization method for shape and topology optimization. Computer *Methods in Applied Mechanics and Engineering*, vol. 93, pp. 291-381.

Tapp, C.; Hansel, W.; Mittelstedt, C.; Becker, W. (2004): Weight-minimization of sandwich structures by a heuristic topology optimization algorithm. *CMES: Computer Modeling in Engineering & Sciences*, Vol. 5, No. 6, pp. 563-574.

Wang, M. Y.; Wang, X.; Guo, D. (2003): A level set method for structural topology optimization. *Computer Methods in Applied Mechanics and Engineering*, vol. 192(1-2), pp. 227-246.

Wang, M. Y.; Wang, X. (2004): "Color" level sets: A multi-phase method for structural topology optimization

with multiple materials. *Computer Methods in Applied Mechanics and Engineering*, vol. 193(6-8), pp. 469 – 496.

Wang, X.; Wang, M. Y.; Guo, D. (2004): Structural shape and topology optimization in a level-set framework of region representation. *Structural and Multidisciplinary Optimization*, vol. 27(1-2), pp. 1-19.

Wang, M. Y.; Zhou, S. (2004): Nonlinear diffusions in structural topology optimization. *Structural and Multidisciplinary Optimization*, published online and in press.

Appendix A: Material and Shape Derivatives

We present a brief description of the material and shape derivatives relevant to the work discussed in the paper with the following materials adapted from (Haug *et al.* (1986)):

Definition: For a given velocity vector $V(x)$ in the shape transformation (17), the *material derivative* $\dot{u}(x;V)$ of $u(x;V)$ for $x \in \Omega$ is defined by

$$\dot{u}(x;V) = \lim_{t\to 0} \frac{1}{t}\left[u(x+tV) - u(x)\right]$$

Lemma 1: For a regular function $f(x)$ defined on Ω, with an integral over Ω defined by

$$\psi_1 = \int_\Omega f(x)\, d\Omega$$

the material derivative of ψ_1 at Ω is given by

$$\psi_1' = \int_\Omega f'(x)\, d\Omega + \int_\Gamma f(x)\,(V\cdot n)\, d\Gamma$$

where $\Gamma = \partial\Omega$ and n is the unit normal to the infinitesimal area $d\Gamma$.

Lemma 2: Consider an integral over Γ,

$$\psi_2 = \int_\Gamma g(x)\, d\Gamma$$

where $g(x)$ is a regular scalar function defined on Γ. Then the material derivative of ψ_2 at Ω is given by

$$\psi_2' = \int_\Gamma g'(x)\, d\Gamma + \int_\Gamma \left(\nabla g\cdot n + \kappa g(x)\right)(V\cdot n)\, d\Gamma$$

where $\kappa = \operatorname{div} n = \nabla\cdot n$ is the curvature of Γ in R^2 and twice the mean curvature of Γ in R^3.

Lemma 3: Consider an integral over Γ,

$$\psi_3 = \int_\Gamma g(x)\cdot n\, d\Gamma$$

where $g(x)$ is a regular vector function defined on Γ and n is the normal vector of Γ. Then the material derivative of ψ_3 at Ω is given by

$$\psi_3' = \int_\Gamma \left(g'(x)\cdot n + \operatorname{div} g(x)\ \ (V\cdot n)\right) d\Gamma$$